Active current-limiting control to handle DC line fault of overhead DC grid

MENG Zhou[1], WANG Xiang[1], WENPING Zuo[1], WEIXING Lin[2], JINYU Wen[1],

RUIZHANG Yang[1] , BINYE Ni[1], XIAOJUN Lu[1]

[1] State Key Laboratory of Advanced Electromagnetic Engineering and Technology (Huazhong University of Science and Technology), Wuhan 430074, Hubei Province, China
[2] TBEA China Xinjiang Sunoasis Co., Ltd, Urumqi 830011, Xinjiang Province, China

Abstract-- **To handle with the DC line faults in a DC grid, this paper proposed an active current-limiting controller for hybrid MMC. With this active current-limiting control strategy, the requirement of interruption current of DCCB will be significantly decreased, and the investment of DC grid will be reduced obviously. Firstly, the control architecture of active current-limiting controller is disclosed. To avoid the overvoltage of submodule capacitors during DC fault, a dynamic limiter for the reference value of the DC current controller is proposed. To decrease the peak of fault current, the feedforward controller of DC voltage is put forward. The decoupling controllability of the AC/DC voltage of hybrid MMC is disclosed. The current-limiting mechanism of the active current-limiting controller is analysis. Then, the validity of the active current-limiting control strategy is verified by RTDS.**

Index Terms—**DC grid, DC fault, Hybrid MMC, Active current-limiting control.**

I. INTRODUCTION

DC grid has a good application prospect in integration, transmission, and grid-connection of the large-scale wind power and photovoltaic. Due to the necessity for large-scale development and utilization of offshore wind power and photovoltaic, the technical requirements of DC grid using the overhead lines are more urgent [1]-[2]. Compared with the cable, the probability of short-circuit fault of the overhead line increases significantly.

At present, the methods to handle the fault of the overhead line in the DC grid are to isolate fault passively by high-speed and large-interruption capacity DC circuit breaker (DCCB) [3]-[5]. Once short-circuit fault on DC line, the fault current that is several times higher than rated current must be interrupted within 5ms [6]. However, it is challenging to develop a high-speed and large-interruption capacity DCCB to meet the above requirements. Whether it is a hybrid DCCB or a mechanical DCCB, its effectiveness and reliability still need to be verified by HVDC engineering. Crucially, even if the functionalities and performance of DCCBs meet the requirements, it is still very costly. The DC grid is uneconomic because of a large amount of DCCBs has been implemented, which make it challenging to popularize and application of DC grid.

Another way to handle the DC fault is to use the converter with fault blocking function[7]-[9], such as the hybrid MMC consisting of a half bridge sub-module (HBSM) and full bridge sub-module (FBSM) or clamp double sub-modules (CDSM). Once the fault occurs, all converters are blocked to isolate the fault current. The DC grid is isolated from the AC grid during the blocking of the converters, and the restart process of the DC grid is complicated, resulting in relatively long power recovery time, which may lead to the problem of stability of the AC system.

In terms of the protection methods for the DC lines fault, a non-unit fault protection principle based on the initial wave as well as the reflected waves to improve the protection sensitivity in high impedance faults is proposed in [13]. A new whole-line quick-action protection principle for HVDC transmission lines is presented in [14]. Besides, there are many protection methods for the DC lines fault are discovered in [15]-[17].

New approaches are urgently required to deal with the overhead line fault of the DC grid. Many current-limiting control strategies without blocking the converter are proposed in [10]-[12]. To ride through a pole-to-ground dc fault without bringing dc bias at the neutral point of the interface transformer, a pole-to-ground dc fault ride through strategy is proposed in [11]. The proposed control scheme enables a monopole symmetrical hybrid MMC-HVDC system to behave like a bi-pole system, thus provides an attractive approach with high robustness and system availability for applications in future HVDC systems.

As for the hybrid MMC composed of the HBSM and FBSM, the advanced control strategy can be designed to achieve the purpose of active current-limiting of fault current during the DC fault, supplemented by the DCCB with slow interruption speed and low interruption capacity to clear the DC fault.

An active current-limiting control strategy to handle DC fault of overhead line in the DC grid is proposed in the paper. The decoupling controllability of the AC/DC voltage of hybrid MMC is disclosed. The current-limiting mechanism of the active current-limiting controller is analysis. The effectiveness and feasibility of the control strategy are verified by the RTDS.
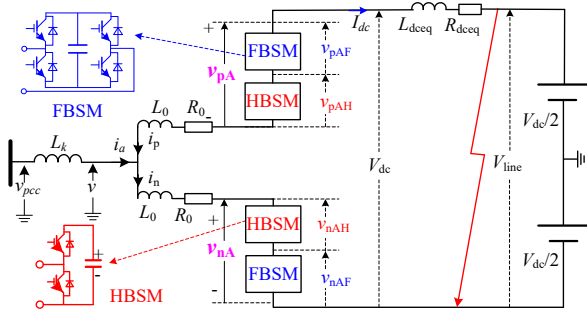
Fig. 1 The single-phase topology of hybrid MMC

II. THE DECOUPLING CONTROLLABILITY OF THE AC/DC VOLTAGE OF THE HYBRID MMC

The single-phase topology of hybrid MMC is shown in Fig. 1, and its arm bridge is composed of N_F full bridge submodule (FBSM) and N_H half bridge submodule (HBSM) connected in series. To simplify the analysis, $N_F = N_H$ is taken in this paper. R_0 and L_0 are the equivalent inductance and equivalent resistance of bridge arm, respectively. The AC output voltage of the hybrid MMC is defined as:

$$v = M_{ac} \frac{V_{dcn}}{2} \cos(\omega t + \theta_v) \qquad (1)$$

Where, M_{ac} is the AC modulation ratio. V_{dcn} is rated DC voltage. θ_v is the phase difference between the AC output voltage of hybrid MMC and the voltage of Point of Common Coupling (PCC). The voltage across the R_0 and L_0 are ignored when the MMC operated in steady-state. Then the voltage across the upper bridge arms and the lower bridge arms, respectively, can be expressed as:

$$\begin{aligned} v_p &= V_{dc}/2 - v \\ v_n &= V_{dc}/2 + v \end{aligned} \qquad (2)$$

Where, V_{dc} is DC voltage. It is assumed that the number of inserted submodules of the upper and lower bridge arm at a specific moment is N_p and N_n, respectively. And it is considered that the voltage sharing algorithm for the submodule capacitor is suitable, and the average voltage

of all submodules capacitor is denoted as V_{cavg}. If the fluctuation of the submodule capacitor voltage is ignored (generally less than 5%), then the V_{dc} can be obtained from (2),

$$V_{dc} = v_p + v_n = (N_p + N_n)V_{cavg} \qquad (3)$$

It can be seen from (3) that V_{dc} can be adjusted by controlling $(N_p + N_n)$ when V_{cavg} remains constant. M_{dc} is defined as dc modulation ratio. The V_{armdc} is defined as the dc component of the sum of the capacitance voltages of all sub-modules in the bridge arm unit, hereinafter referred to as bridge arm capacitance voltage, which represents the energy storage of the bridge arm unit. V_{dc} is further expressed as:

$$\begin{cases} V_{dc} = M_{dc}V_{armdc} = M_{dc}\left(N_{sm}V_{cavg}\right) \\ V_{armdc} = \frac{1}{6}\sum_{A,B,C}\sum_{p,n}\sum_{1}^{N_{sm}}V_{ci\_dc} \approx \frac{1}{6}\sum_{A,B,C}\sum_{p,n}\sum_{1}^{N_{sm}}V_{cavg} \end{cases} \qquad (4)$$

Where, N_{sm} is the number of submodules in the bridge arm. V_{ci_dc} is the DC component of the voltage of submodule capacitor. When the number of HBSM equals to the number of FBSM in the arm bridge, the range of dynamic adjustment for M_{dc} is [-0.1, 1.0]. Therefore, the output range of V_{armdc} is [-0.1V_{dcn}, V_{dcn}]. According to equation (4), if the V_{armdc} is controlled to V_{dcn}, the V_{dc} is variable by adjusting the M_{dc}. Formula (1) can be further expressed as

$$v = M_{ac} \frac{M_{dc}V_{armdc}}{2} \cos(\omega t + \theta_v) \qquad (5)$$

According to equation (4), when the V_{armdc} is controlled around the V_{dcn}, the output voltage V_{dc} of the hybrid MMC is determined by M_{dc}. And the range of dynamic regulation of M_{dc} depends on the number ratio between HBSM and FBSM in the arm bridge. Mac determines AC output voltage v. Therefore, equations (4) and (5) represent the decoupling controllability of AC/DC output voltage of hybrid MMC.
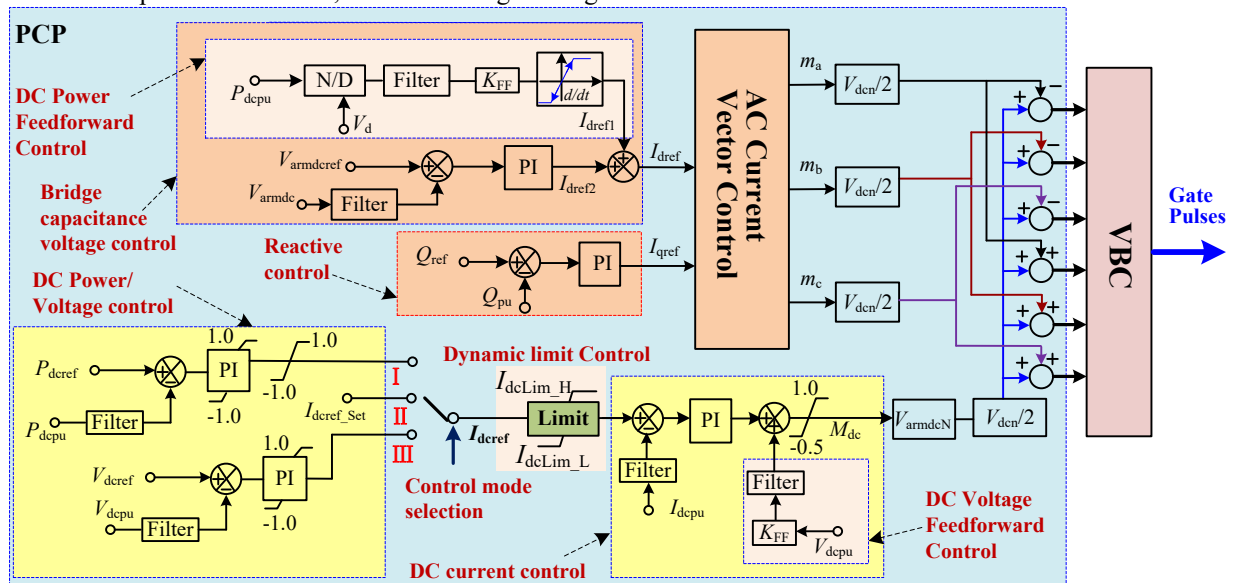

Fig. 2 Active current-limiting control

III. ANALYSIS OF ACTIVE CURRENT-LIMITING CONTROL MECHANISM OF HYBRID MMC

For the single converter shown in Fig. 1, The line voltage V_{line} drops to zero (only the metallic short circuit fault is considered in this paper) after the fault occurs. The control strategy of power station switches to the DC current control directly after the delay time of hundreds of microseconds When DC fault is detected. The DC bus voltage, V_{dc}, of the converter will be damping to zero nonlinearly since the DC current controller. And the decay process of DC voltage typically remains from milliseconds to tens of milliseconds (depending on the time constant of DC current control loop). The converter will inject continuously the short-circuit current, I_{dc}, to the fault position before the V_{dc} drops to zero. I_{dc} reaches peaks when V_{dc} equals V_{line}. Due to a large number of converter stations in the DC grid, high fault current will be detected in the fault line during the fault. It will increase significantly the interruption capacity of DCCB located in the faulted lines. If the electrical parameters in the fault loop remain constant, the faster the V_{dc} decreases to zero, the lower the peak value of I_{dc}. Therefore, by adding the feedforward controller of V_{dc} in DC current controller, the active current-limiting control, as shown in Fig. 2 can accelerate the attenuation rate of V_{dc} and reduce the peak value of DC current in faulted line. And thereby reduce the requirement of interruption capacity of DCCB.

The DC current controller diagram can be obtained when the DC voltage feedforward controller is taken into account, as shown in Fig. 3. The s-domain expression of the DC current i_{dc} is

$$I_{dc}(s) = G_1(s)I_{dcref} - G_2(s)V_{line} + G_3(s)V_{dc} \qquad (6)$$

$$G_1(s) = \frac{(sk_{pi} + k_{ii})V_{armdcN}I_{dcN}}{s^2LI_{dcN} + s(k_{pi}V_{armdcN} + RI_{dcN}) + k_{ii}V_{armdcN}} \qquad (7)$$

$$G_2(s) = \frac{sI_{dcN}}{s^2LI_{dcN} + s(k_{pi}V_{armdcN} + RI_{dcN}) + k_{ii}V_{dcN}} \qquad (8)$$

$$G_3(s) = \frac{sI_{dcN}V_{armdcN}k_{FF}}{s^2LI_{dcN} + s(k_{pi}V_{armdcN} + RI_{dcN}) + k_{ii}V_{dcN}} \qquad (9)$$

where, $L=L_{dc}+2L_{arm}/3$, and $R=R_{dc}+2R_{arm}/3$. L_{dc} and R_{dc} represent the total inductance and its equivalent resistance respectively, and L_{arm} and R_{arm} represent the arm bridge inductance and its equivalent resistance respectively. It can be seen from (6) that I_{dc} actually consists of three parts: steady-state component ($G_1(s)I_{dcref}$), fault component ($-G_2(s)V_{line}$) and feedforward component ($G_3(s) V_{dc}$). After the DC fault, the V_{line} decreases to zero, while the V_{dc} decay nonlinearly to zero after the delay time of several ms. The $G_1(s)Idcref$ is determined by the operating state of the DC grid before DC fault. The $-G_2(s)V_{line}$ is determined by the dynamic characteristics of V_{line}. The V_{dc} and V_{line} have similar attenuation characteristics after the fault. By comparison (8) and (9) , it can be seen that the size of the fault component and feedforward component is relatively close if the

feedforward coefficient of K_{FF} is 0.95 and the difference of dynamic characteristics between V_{dc} and V_{line} is ignored. It can be considered that the feedforward component will offset part of the fault component, thus reducing the DC overcurrent peak after the fault.
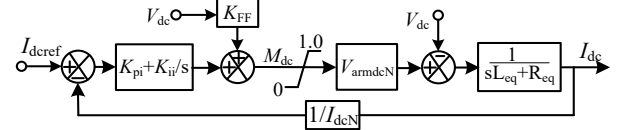

Fig. 3 DC current control block with DC voltage feedforward controller

IV. SIMULATION VERIFICATION

To verify the performance of the active current limiting controller, a unipolar converter test system as shown in Fig. 4 is established. The arm of the hybrid MMC contains 95 HBSM and 95 FBSM. The length of the overhead line based on Frequency dependent model is 103km. The parameters of the simulation system are shown in TABLE 1. The hybrid MMC transfers 1.5GW DC power to the V_{dc2} in steady-state. The permanent pole to pole metallicity short-circuits fault that located in 103km from the DC bus is applied at the moment of 2s.
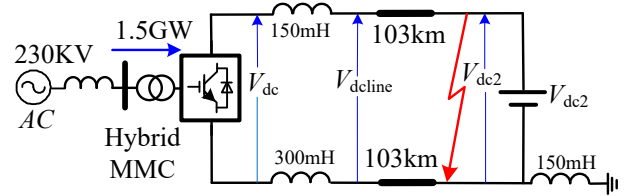

Fig. 4   Simulation system based on Hybrid MMC

TABLE 2

PARAMETERS FOR REAL TIME SIMULATION

| parameters	rated value
MMC rated capacity	1.5GW
Rated DC voltage (V_{dc2})	500 KV
Rated voltage of AC system	230 KV
transformer ratio	230KV/290KV
Bridge arm inductance	15mH
Submodule capacitance value	15μF
The number of FBSM for each arm	95
The number of HBSM for each arm	95

Fig. 5 (a) shows the reference value, I_{dcref}, and the actual value of DC current, I_{dcpu}, during the DC fault. Once the DC fault is detected, the DC outer loop switches from DC power control mode to direct current control mode. After 0.5s, I_{dcref} reduces from 1.0pu to 0. It can be seen that I_{dcpu} can track the target control curve of I_{dcref}, and the DC overcurrent is less than 25% during the current limiting control.

Fig. 5 (b) shows the upper and lower arm currents of phase A. After the DC fault, the DC power is reduced to zero. To maintain the balance of the active power of arm and prevent the overvoltage of the sub-module capacitor, the AC current controller will reduce the active current reference, thus reducing the active power absorbed by the converter from the AC system. Therefore, the base frequency component of the arm current will rapidly decrease to zero. Meanwhile, the DC component of the current of arm bridge decreases with the reduction of the

DC current. Fig. 5 (b) shows that it has almost no obvious overcurrent for the current of the arm during the DC fault.
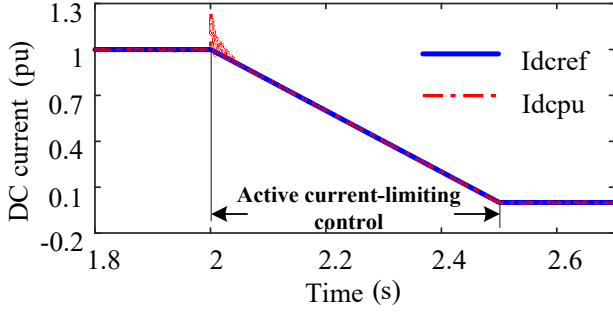
(a) The actual value and reference value of DC current
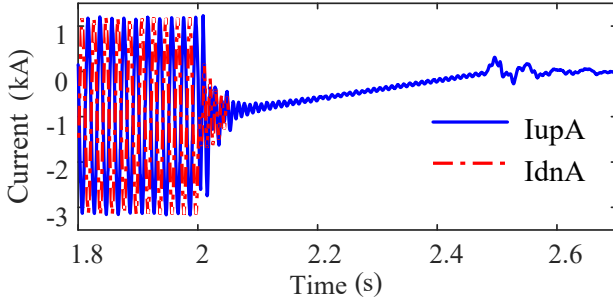
(b) the current in upper and lower arm

Fig. 5 Dynamic characteristics of single converter during the fault

V. REAL-TIME SIMULATION VERIFICATION OF ACTIVE CURRENT -LIMITING CONTROL BASED ON RTDS

To verify the effectiveness of the active current-limiting control, a real-time simulation experiment platform based on RTDS is established of hybrid MMC-HVDC. RTDS is used to simulate the main circuit of the system. The pole control cabinet and the valve control cabinet are used to realize the pole control and the valve control algorithm. The man-machine interaction system is used to issue the control instructions, as well as to monitor the system operation condition and call operation data. Fig. 7 shows the schematic diagram of the main circuit of the system. Table 3 shows the parameters of the system. MMC1 controls DC power, MMC2 controls DC voltage. t=0.2s, AC circuit breaker BRK is closed to simulate the permanent bipolar short-circuit fault. Fig. 8 shows the experiment results of MMC1 and MMC2.

TABLE 3
PARAMETERS FOR REAL TIME SIMULATION

| parameters	rated value
MMC rated capacity	10MW
Rated DC voltage (Vdcn)	±10kV
Rated voltage of AC system	10 kV
transformer ratio	10kV/10kV
Bridge arm inductance	12mH
Submodule capacitance value	3360μF
Delay time of controller	200us
Rated voltage of submodule capacitance	0.833 kV
DC limiting-current inductance	32.8mH
The number of FBSM for each arm	12
The number of HBSM for each arm	12
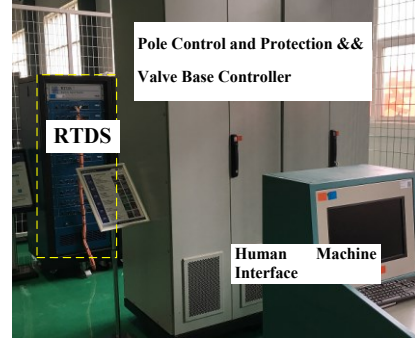
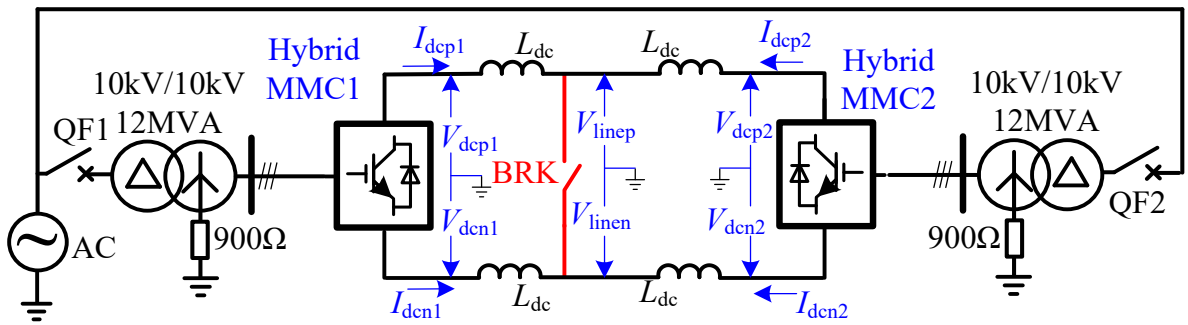Fig. 6 The photo of real time simulation system.

Fig. 7 Main circuit principle diagram of real time simulation system.

When the pole controller and protection (PCP) of MMC1 detects the drops of DC voltage, the DC voltage feedforward controller reduces rapidly the dc voltage modulation ratio M_{dc}, thus reducing the DC bus voltage (V_{dcp1}, V_{dcp2}) of MMC1 to adopt the external dc voltage (V_{linep}, V_{linen}).

It can be seen that the AC current (I_{a1}, I_{b1}, I_{c1}) at the valve side of the converter valve and the current of a-phase upper and lower bridge arms (I_{ap1}, I_{an1}) had no obvious overcurrent after the fault. At the same time, the voltage of the sub-module capacitance has no obvious overvoltage. once the active current feedforward controller detects the drop of DC power P_{dcpu}, it will reduce the active current instruction Idcref1, resulting in the reduction of the total active current instruction I_{dcref}, thus reducing the active power absorbed by MMC1 from the ac system and reducing the capacitance overvoltage level of the sub-module.

As the delay of PCP (approximately 50us) makes M_{dc} unable to respond to the change of external DC voltage in real time, the dc current (I_{dcp1}, I_{dcn1}) appears a certain overcurrent, and its peak value is within 1.5pu. During the process of dc fault current (I_{dcp1}) rising to the peak and starting to decline, the dc bus voltage (V_{dcp1}) appears negative value due to the reversal of voltage direction at both ends of the current-limiting inductance L_{dc}. V_{dcp1} gradually returns to zero after I_{dcp1} reaches steady state.
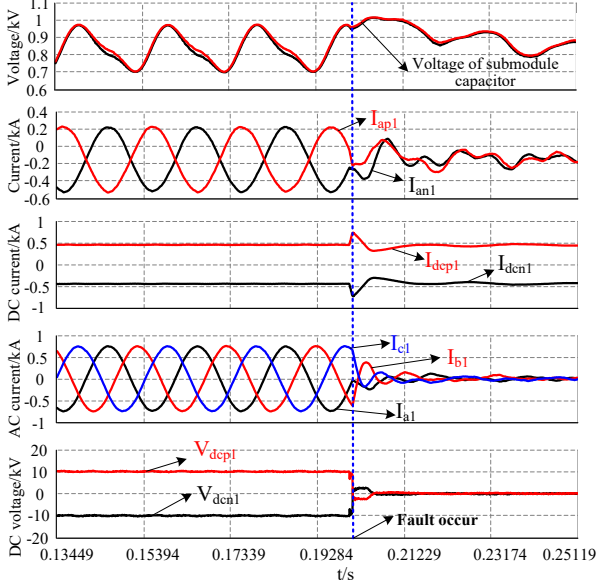

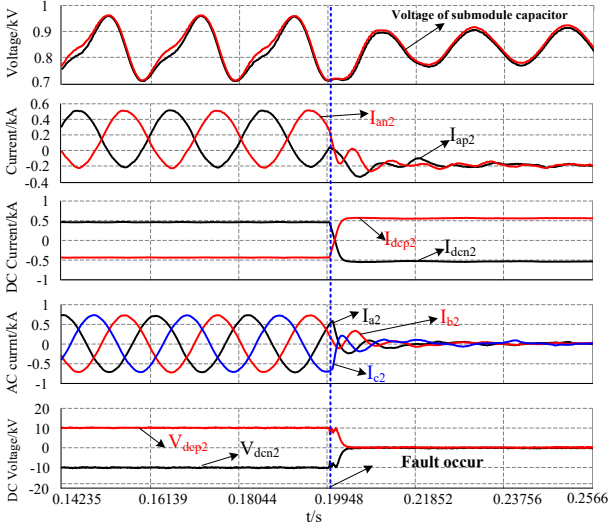Fig. 8 The experimental results of MMC1

Fig. 9 The experimental results of MMC2

VI. Conclusions

An active current-limiting control strategy to handle DC fault of overhead line in the DC grid is proposed in the paper. By adding the feedforward controller of V_{dc} in DC current controller, the active current-limiting control can accelerate the attenuation rate of the DC voltage and reduce the peak value of DC current in the faulted line. And thereby reduce the requirement of interruption capacity of DCCB. The effectiveness and feasibility of the control strategy are verified by the RTDS.

VII. Acknowledgements

References

[1] ABB, DolWin2-900 MW HVDC Light Transmission-The world's largest wind power grid connection, Accessed at http://search.abb.com/library/Download.aspx? DocumentID=POW0075&LanguageCode=en&DocumentPartId=& Action=Launch on 29.06.2012

[2] A. Abdalrahman, E. Isabegovic, DolWin1 - Challenges of connecting offshore wind farms[C]. 2016 IEEE International Energy Conference (ENERGYCON) Leuven, 2016, pp. 1-10.

[3] C C Davidson, R S Whitehouse, C D Barker, J. P. Dupraz and W. Grieshaber. A new ultrafast HVDC Circuit breaker for meshed DC networks [C]. 11th IET Inter. Conf. on AC and DC Power Transm. Birmingham, 2015, pp. 1-7.

[4] J Häfner, B Jacobson. Proactive Hybrid HVDC Breakers-A key innovation for reliable HVDC grids[C]. CIGRE, pp. 1-9, 2011.

[5] W Lin, D Jovcic, S Nguefeu, H Saad. Modelling of high-power hybrid DC circuit break-er for grid-level studies [J]. IET Power Electronics, vol. 9, no. 2, pp. 237-246, 10 2 2016.

[6] CIGRE WG A3/B4.34. Technical requirements and specifications of state-of-the-art HVDC switching equipment[C]. CIGRE technical brochure 683, Paris, April 2017.

[7] Xiang W, Lin W, An T, et al. Equivalent electromagnetic transient simulation model and fast recovery control of overhead VSC-HVDC based on SB-MMC [J]. IEEE Transactions on Power Delivery, 2017, 32(2): 778-788.

[8] Y Xue, Z Xu, G Tang. Self-Start Control with Grouping Sequentially Precharge for the C-MMC-Based HVDC System [J]. IEEE Transactions on Power Delivery, vol. 29, no. 1, pp. 187-198, Feb. 2014.

[9] R Marquardt. Modular multilevel converter: an universal concept for HVDC-networks and extended DC-bus-applications[C]. Proc. Power Electron. Conf. Int., pp. 502-507, 2010.

[10] W Lin, D Jovcic, S Nguefeu, H Saad. Full-Bridge MMC Converter Optimal Design to HVDC Operational Requirements [J]. IEEE Transactions on Power Delivery, vol. 31, no. 3, pp. 1342-1350, June 2016.

[11] W Xiang, W Lin, L Xu, J Wen. Enhanced Independent Pole Control of Hybrid MMC-HVDC System [J]. IEEE Transactions on Power Delivery, vol. PP, no. 99, pp. 1-1. doi: 10.1109/TPWRD.2017.2715040.

[12] J Hu, K Xu, L Lin, R Zeng. Analysis and Enhanced Control of Hybrid-MMC-Based HVDC Systems during Asymmetrical DC Voltage Faults [J]. IEEE Transactions on Power Delivery, vol. 32, no. 3, pp. 1394-1403, June 2017.

[13] Shuxin Luo, Xinzhou Dong, Shenxing Shi and Bin Wang, "A non-unit protection principle based on travelling wave for HVDC transmission lines," 2015 50th International Universities Power Engineering Conference (UPEC), Stoke on Trent, 2015, pp. 1-6.

[14] G. Song, X. Chu, S. Gao, X. Kang and Z. Jiao, "A New Whole-Line Quick-Action Protection Principle for HVDC Transmission Lines Using One-End Current," 2018 IEEE Power & Energy Society General Meeting (PESGM), Portland, OR, 2018, pp. 1-1.

[15] F. Kong and B. Zhang, "A novel disturbance identification method based on empirical mode decomposition for HVDC transmission line protection," 12th IET International Conference on Developments in Power System Protection (DPSP 2014), Copenhagen, 2014, pp. 1-6.

[16] J. Suonan, J. Zhang, Z. Jiao, L. Yang and G. Song, "Distance Protection for HVDC Transmission Lines Considering Frequency-Dependent Parameters," in IEEE Transactions on Power Delivery, vol. 28, no. 2, pp. 723-732, April 2013.

[17] Zhao Li, G. Zou, Bingbing Tong, H. Gao and Qian Feng, "Novel traveling wave protection method for high voltage DC transmission line," 2015 IEEE Power & Energy Society General Meeting, Denver, CO, 2015, pp. 1-5.

[18]